

# A global three-dimensional time-dependent lightning source of tropospheric NO<sub>x</sub>

H. Levy II and W. J. Moxim

NOAA Geophysical Fluid Dynamics Laboratory, Princeton University, Princeton, New Jersey

P. S. Kasibhatla<sup>1</sup>

MCNC, Environmental Programs, Research Triangle Park, North Carolina

**Abstract.** The spatial and temporal distribution for a global three-dimensional, time-dependent lightning source of NO<sub>x</sub> is constructed from a general circulation model's (GCM) deep moist convection statistics [Manabe *et al.*, 1974; Manabe and Holloway, 1975], observations of cloud-to-cloud and intracloud lightning fractions and the vertical distribution of lightning discharge [Proctor, 1991], and empirical/theoretical estimates of relative lightning frequency resulting from deep moist convection over ocean and over land [Price and Rind, 1992]. We then bracket the annual global emission of NO<sub>x</sub> from lightning between 2 and 6 Tg N/yr, with a most probable range of 3 to 5 Tg N/yr, by comparing tropospheric NO<sub>x</sub> simulations from the Geophysical Fluid Dynamics Laboratory Global Chemical Transport Model with measurements of NO<sub>x</sub> and/or NO<sub>y</sub> in the mid and upper troposphere where lightning is a major, if not the dominant, source. With this approach, the global magnitude of the lightning source is constrained by observed levels of NO<sub>x</sub>, while the temporal and spatial distributions of the source are under the control of the parent GCM. Although our lightning source is smaller than many previous estimates, it is still the major source of NO<sub>x</sub> and NO<sub>y</sub> in the mid and upper troposphere for a latitude belt running from 30°N to 30°S, an important contributor to summertime free tropospheric levels over the midlatitudes, and a major contributor, even in the lower troposphere, to the low NO<sub>x</sub> and NO<sub>y</sub> levels over the remote oceans.

## 1. Introduction

NO<sub>x</sub> (NO + NO<sub>2</sub>) plays a key role in tropospheric chemistry [Levy, 1971; Chameides and Walker, 1973; Crutzen, 1974]. With a short tropospheric lifetime (1–10 days) and a number of diverse and dispersed sources, NO<sub>x</sub> mixing ratios range from tens of parts per billion by volume (ppbv) in regions of surface pollution to a few parts per trillion by volume (pptv) in the marine boundary layer (MBL) of the remote central Pacific and are only sparsely measured throughout most of the troposphere [e.g., Logan, 1983; Fehsenfeld *et al.*, 1988; M.A. Carroll and L. Emmons, private communication, 1995]. In the foreseeable future, we do not expect that available measurements and proposed measurement campaigns will allow us to generate the detailed global NO<sub>x</sub> fields needed to study a wide range of questions in global tropospheric chemistry. Rather, we will have to rely on simulated global NO<sub>x</sub> fields that have been generated by global chemical transport models (GCTM) and evaluated with existing NO<sub>x</sub> observations. The key to such simulations, assuming a GCTM with adequate representations of transport, chemistry, and removal, is an accurate estimate of the magnitude, spatial distribution and temporal variability of tropospheric NO<sub>x</sub> sources.

<sup>1</sup>Formerly at School of Earth and Atmospheric Sciences, Georgia Institute of Technology, Atlanta, Georgia.

Copyright 1996 by the American Geophysical Union.

Paper number 96JD02341.  
0148-0227/96/96JD-02341\$09.00

The global distribution, timing, and magnitude of five of the six currently known NO<sub>x</sub> sources are relatively well characterized. They are based on detailed emission inventories and, where possible, simulated nitrate deposition and reactive oxidized nitrogen species concentrations have been compared with observations from regions of the troposphere dominated by an individual source. A sample of the range of their estimated global magnitudes, along with the appropriate references, are given in Table 1. However, the global distribution and timing of the sixth source, NO<sub>x</sub> emissions from lightning discharge, have only been crudely characterized [Hameed *et al.*, 1981; Penner *et al.*, 1991], and previous estimates of the global magnitude, as shown in Table 1, vary widely. These estimates, most of which trace back to a 1925 estimate of global flash frequency [Brooks, 1925] and either first-principles calculations of NO<sub>x</sub> per lightning stroke or atmospheric and/or laboratory measurements of NO<sub>x</sub> in a lightning discharge, range from a few teragrams nitrogen per year up to unrealistic values exceeding 100 Tg N/yr (see Table 2 of Lawrence *et al.*, [1995] for more detail).

After an analysis of previous global source estimates, based both on direct calculations and in situ observations, Liaw *et al.* [1990] proposed 81 Tg N/yr as the best estimate of the global lightning source. A recent study by Lawrence *et al.* [1995] reexamined the direct calculations and arrived at a much lower range of 1–8 Tg N/yr, though it should be noted they were extrapolating globally from a relatively limited number of local measurements.

**Table 1.** Global Sources of NO<sub>x</sub>

Source	Estimated Magnitude, Tg N/yr	Reference
Fossil fuel	22	<i>Hameed and Dignon</i> [1988]
	21.2	<i>Levy and Moxim</i> [1989]
	22.2	<i>Benkovitz et al.</i> [1996]
	21.4	this work
Subsonic aircraft	1	<i>Beck et al.</i> [1992]
	0.45	<i>Wuebbles et al.</i> [1993]
Stratosphere	0.64	<i>Kasibhatla et al.</i> [1991]
Biomass burning	~6	<i>Hao et al.</i> [1989]
	8.5	<i>Levy et al.</i> [1991]
	5.8	<i>Penner et al.</i> [1991]
Soil biogenic emissions	~5	<i>Dignon et al.</i> [1992]
	4.7	<i>Müller</i> [1992]
	5.5	<i>Yienger and Levy</i> [1995]
Lightning	2.1	<i>Hameed et al.</i> [1981]
	19.1 - 152	<i>Liaw et al.</i> [1990]
	3 - 10	<i>Penner et al.</i> [1991]
	220	<i>Franzblau and Popp</i> [1989]
	1 - 8	<i>Lawrence et al.</i> [1995]
	2 - 6	this work

In an earlier global nitrogen budget study, *Logan* [1983] estimated that measurements of nitrate deposition in remote locations far from all other NO<sub>x</sub> sources would support a lightning contribution of no more than 20 Tg N/yr. In their GCTM simulations for January and July, *Penner et al.* [1991] arrived at a similar upper limit. They used a 10°x15° lightning distribution based on observed thunder days and a formula relating, as a function of latitude, thunder days to lightning strokes, though it should be noted that lightning strokes/thunder day can be highly variable. They found that a lightning source of 3-10 Tg N/yr gave reasonable agreement with some observed free tropospheric levels of NO, though they appear to underestimate the upper tropospheric NO maxima observed by *Davis et al.* [1987] off the coast of California and by *Drummond et al.* [1988] over the subtropical and tropical Atlantic. A preliminary GCTM study by *Levy et al.* [1992], which used a very limited set of NO and NO<sub>y</sub> observations in the upper troposphere, bracketed the global lightning source between 2 and 4 Tg N/yr.

Both previous GCTM studies and the *Lawrence et al.* [1995] reanalysis support a global lightning source that is at the low end of past estimates and is approximately 10% of current global NO<sub>x</sub> emission estimates of ~40 Tg N/yr [e.g., *Moxim et al.*, 1994]. However, this emission of NO<sub>x</sub> into the mid and upper troposphere, where it has a relatively long lifetime and other in situ sources are less than 1 Tg N/yr, has the potential to significantly influence the NO<sub>x</sub> levels and the resulting ozone chemistry of that region [*Lin et al.*, 1988; *Trainer et al.*, 1991; A.A. Klonecki, private communication, 1995].

Not only have there been a very wide range of estimated global source strengths, but no ab initio calculations exist to

generate a believable three-dimensional, time-dependent lightning source of NO<sub>x</sub>. All previous approaches, as well as this study, combine numerical models, theory, and observations in the construction of an empirical source. One general approach [e.g., *Price and Rind*, 1992] uses a general circulation model (GCM) to construct global time-dependent maps of lightning and then uses theory and laboratory studies of NO<sub>x</sub> emission per lightning flash to generate the global source of NO<sub>x</sub>. We have taken a more empirical path. In section 2 our GCM is used to construct global time-dependent maps of deep moist convection, and observations and theories of intra-cloud (IC) and cloud-ground (CG) lightning are then used to convert the deep moist convection fields into three-dimensional, time-dependent maps of lightning. In section 3, rather than estimating the NO<sub>x</sub> production per lightning flash from theory and observation, we determine the range of global scaling factors that produces the best fit between our GCTM simulations of NO<sub>x</sub> and NO<sub>y</sub> and observations from regions where lightning is expected to be a major, if not the dominant, contributor. This range of empirically determined global scaling factors then provides our estimated range of global source strengths for the emission of NO<sub>x</sub> by lightning. The reactive nitrogen GCTM, employing a single scaling factor based on a global source strength of 3 Tg N/yr, is then used in section 4 to quantify the contribution of lightning to the levels of NO<sub>x</sub> and NO<sub>y</sub> throughout the troposphere.

## 2. Relative Global Source

Our construction of the relative global lightning source of NO<sub>x</sub> has three stages. In section 2.1 a horizontal time-dependent distribution of deep moist convection is constructed us-

ing GCM statistics [Manabe and Holloway, 1975]. In section 2.2 we use observed vertical distributions of lightning origination and relative intracloud and cloud-ground frequency [Proctor, 1991] and an empirical ratio of lightning flashes in continental and maritime convection [Price and Rind, 1992] to convert the two-dimensional distribution of deep moist convection to a three-dimensional distribution of IC and CG lightning. The conversion of our lightning distribution to a relative distribution of NO<sub>x</sub> emission then requires a number of simplifying approximations and estimates of the energy in CG and IC flashes.

### 2.1. Horizontal and Temporal Distribution of Lightning

Our horizontal and temporal distributions of lightning begin with simulated moist convection statistics, which are sampled once every 6 hours from a year's integration of a GCM with a horizontal resolution of ~265 km, 11 vertical levels (standard pressures of 990, 940, 835, 685, 500, 315, 190, 110, 65, 38, and 10 mbar), and no diurnal cycle [Manabe et al., 1974; Manabe and Holloway, 1975]. While the model's resolution cannot resolve individual convective cells or even large mesoscale weather systems and their associated high-frequency lightning [c.g., Goodman and MacGorman, 1986], it will be shown that the model's seasonally varying regional distribution of convection adequately captures the observed global patterns of lightning. For the model's convective event to generate lightning, we require that saturated convection occur contiguously from ~800 mbar to at least 400 mbar. In this way we guarantee that the resulting NO<sub>x</sub> emission by lightning will be directly coupled to the strong convective transport and mixing in the model.

Guided by the empirical analysis of Price and Rind [1992], deep moist convective events over the ocean, which are much less likely to generate lightning, are weighted by 0.1, except for the grid boxes containing the Caribbean Islands and Indonesia, which are treated as land points and given a weight of 1.0. Because of the model's lack of summertime precipitation over the southeastern U.S. and parts of eastern Asia and Australia, these regions, which are convective and which are known to generate a great deal of summertime lightning in the real world, do not satisfy our criteria (see the preceding paragraph) for convectively generated lightning in the model. Therefore we supplement moist convective events with dry convection in those regions. These supplemental dry convective events, which amount to ~4% of the total convective events sampled during the year, are then scaled by 0.75 to improve the agreement between the model's distribution of convection and the observed latitudinal distributions of lightning.

Implicit in relating deep moist convection frequency directly to lightning frequency is the assumption that all deep convective events, after the various empirical scalings, have the same flash intensity. Clearly, this is not strictly correct, as a number of theoretical and empirical studies have shown [see Price and Rind, 1992, and references therein], but it is a necessary simplification for this study. In the future, a logical extension would be to relate the flash intensity to the intensity of the individual convective events.

In Figure 1 the yearly averaged latitudinal distribution of the GCM's saturated deep convection frequency is compared with the observed yearly averaged latitudinal distribution of lightning flashes assembled by Turman and Edgar [1982] for dawn and dusk and by Orville and Spencer [1979] for dusk and midnight. In order to focus on the relative latitude distri-

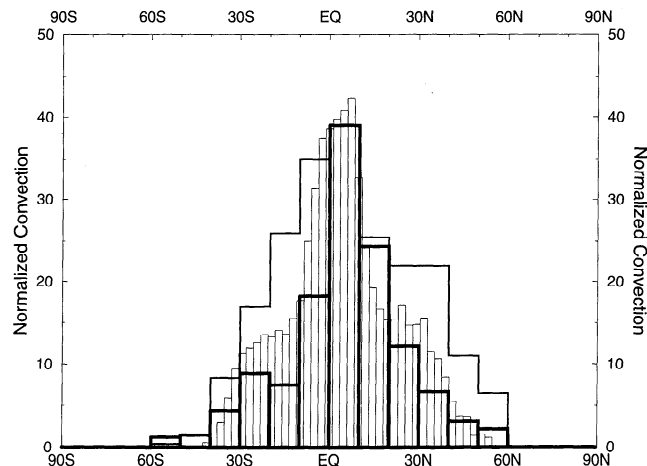


Figure 1. The simulated annual latitudinal distribution of deep convection is represented by the narrow bars. The heavy wide bars are the Orville and Spencer [1979] observations of annual latitudinal distribution of lightning flashes, and the thin wide bars are the Turman and Edgar [1982] observations. All three distributions have been scaled to give the same number for the 0°-10°N band.

butions and to allow a direct comparison between saturated deep convection frequency and flash frequency, all three distributions are scaled to give the same number for the 0°-10°N band. Given the prevalence of year-round convection in the tropics and strong summer convection over the continents in the summer, the observed distributions in Figure 1 come as no surprise. Both measured and simulated distributions are concentrated between 20°N and 20°S with significant secondary contributions between 20°-40°N and 20°-40°S, a sharp drop-off poleward of 40°, and almost nothing poleward of 60°. In general, the simulated convective frequency falls between the two observed lightning distributions and captures the observed latitudinal distribution.

In Figure 2 we show the winter, summer, and annual simulated latitude-longitude distributions of saturated deep convection frequency, which are considerably more complex than those in Figure 1. Note that the marine deep convection has been scaled by 0.1. The convection/lightning, which is clearly not uniformly distributed for a given latitude, is concentrated over land with a smaller, though not insignificant contribution over the tropical ocean. At midlatitudes the continental-based lightning occurs almost exclusively in the summer. In the tropics, the lightning migrates with the tropical rainy season over South America and Africa and with the movement of the Asian monsoon from the Indian subcontinent and Southeast Asia in the summer to Indonesia and northern Australia in the winter. Over the ocean, there are weaker maxima stretching down to 30°S in the western South Pacific throughout the year, off the east coast of the United States and Asia in the summer, and over the tropical Indian Ocean. A weak band of lightning observed over the wintertime North Pacific and Atlantic (S.J. Goodman, private communication, 1996) is not present in the simulation. While there are significant year-to-year variations in regional lightning intensity (see Goodman and Christian [1993] for a recent discussion), these simulated spatial patterns and their relative intensities are generally in good agreement with the seasonal and annual global lightning frequency maps of Orville and Henderson [1986], Turman and Edgar [1982], and Goodman and Christian [1993].

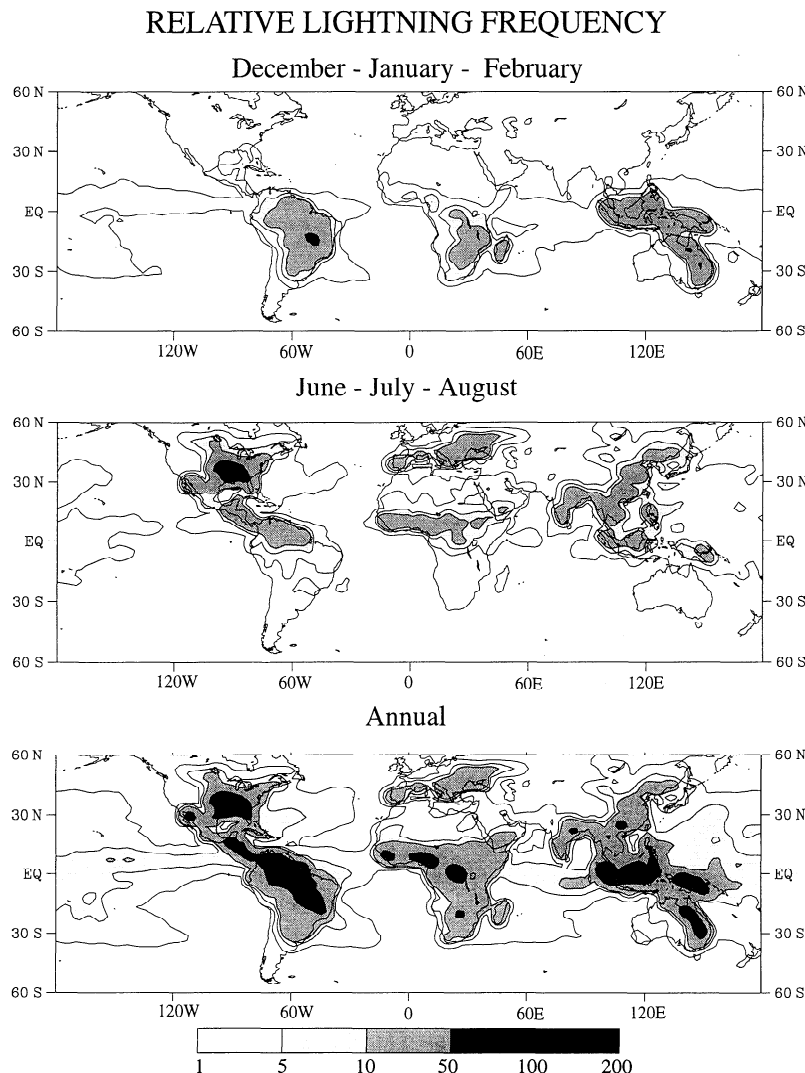


Figure 2. The simulated summer, winter, and annual distribution of deep convection, based on a once every 6 hours sample of the model's convection statistics. The actual numbers represent the number of 6-hour periods with convection occurring. This number can be linearly related to flash frequency if all deep convective events are assumed to have the same number of flashes.

## 2.2. Vertical Distribution of Lightning and NO<sub>x</sub> emission

To determine the vertical distribution of NO<sub>x</sub> emission for a given event, we must first generate the vertical distribution of intracloud and cloud-to-ground lightning. While it may be possible to do so from physical properties predicted by those GCMs with subgrid-scale parameterizations of clouds and moist convection [e.g., Price and Rind, 1993], we have chosen an empirical route. Our vertical distribution is based on the analysis of Proctor [1991], who monitored 773 lightning flashes in South Africa and determined both the vertical distribution of lightning flash origin and the vertical distribution the CG and IC fractions. The 13 thunderstorms over a 10-year period yielded a clear bimodal distribution with flash origination maxima at ~500 mbar and ~300mbar and a CG fraction of 0.28. The CG flashes originated almost completely in the lower maximum (~500 mbar), and the IC flashes, while distributed throughout, occurred primarily in the upper maximum (~300mbar). Contrary to a number of previous studies that argued for a strong latitude dependence in the CG frac-

tion, a recent analysis of cloud and lightning data by Price and Rind [1993] argues that the fraction varies only between 0.24 and 0.28 over the latitude range of 0°- 40°. Therefore we have chosen to use the Proctor [1991] distributions of IC and CG for all latitudes.

For the final conversion to a time-dependent, three-dimensional source of NO<sub>x</sub>, we make two further simplifications: All CG lightning flashes produce the same amount of NO<sub>x</sub> (CG<sub>NO<sub>x</sub></sub>), which is linearly apportioned among the levels according to their mass; NO<sub>x</sub> production by IC lightning (IC<sub>NO<sub>x</sub></sub>) is also the same for all flashes and remains within the model layer of origination. The approximation of the same NO<sub>x</sub> production for all IC and for all CG flashes is related to the earlier approximation of the same flash frequency for all convective events and results from the same lack of model-generated convective intensity data. There are also two implied assumptions: NO<sub>x</sub> production varies linearly with the flash energy, and NO<sub>x</sub> production is independent of pressure over the range 1000 mbar-200 mbar. Holmes *et al.* [1971] found that CG flashes contained at least 3 times the energy of

IC flashes, and *Kowalczyk and Bauer* [1982] adopted a factor of 10, which gives an NO<sub>x</sub> flash yield in agreement with both theory and laboratory measurements [*Lawrence*, 1995]. Recently, on the basis of calculations by *Cooray* [1996] that find similar levels of energy dissipation in CG and IC flashes, L. Gallardo (private communication, 1995) has argued that CG and IC flashes produce similar levels of NO<sub>x</sub>.

Two vertical distributions for the percentage production of NO<sub>x</sub> are shown in Figure 3. Case a, which was used in the preliminary study by *Levy et al.* [1992], has IC<sub>NO<sub>x</sub></sub> = CG<sub>NO<sub>x</sub></sub>. IC flashes dominate NO<sub>x</sub> production and maximize NO<sub>x</sub> emission in the upper troposphere with 48% above 7 km, 42% between 7 and 2 km, and only 10% below 2 km. Case b, which has CG<sub>NO<sub>x</sub></sub> = 10xIC<sub>NO<sub>x</sub></sub>, will be used in our current calculations. It produces a maximum NO<sub>x</sub> emission in the middle troposphere with only 16% above 7 km, 54% between 7 and 2 km, and 30% below 2 km. While case b will deposit ~3 times more NO<sub>x</sub> in the continental boundary layer, where it may be subject to rapid loss, both distributions emit most of the NO<sub>x</sub> in the free troposphere. This fact, when coupled with lightning's occurrence in a region of upward vertical motion, greatly reduces the impact of the factor of 10 change in the relative NO<sub>x</sub> production by IC and CG lightning.

### 3. Absolute Global Source

Having generated our three-dimensional, time-dependent relative distribution of NO<sub>x</sub> emissions by lightning, we still need to quantify the yearly global source strength. We do so by comparing NO<sub>x</sub> and NO<sub>y</sub> simulated by our GCTM with available observations from regions, primarily the middle and upper troposphere between 30°S and 30°N, that are dominated or at least strongly affected by emissions from lightning. Before examining the data comparison and the calculations of the global lightning source in section 3.2, we should briefly discuss our reactive nitrogen GCTM.

#### 3.1. GCTM Description

The Geophysical Fluid Dynamics Laboratory (GFDL) GCTM is driven by 12 months of 6-hour time-averaged wind, temperature, and precipitation fields from a GFDL GCM [*Mahlman and Moxim*, 1978]. The GCTM has the same horizontal and vertical resolution as the parent GCM and includes parameterizations of horizontal subgrid-scale transport and vertical mixing by dry and moist convection (for details, see Appendix A of *Levy et al.* [1982], and section 2 of *Kasibhatla et al.* [1993]).

The GCTM explicitly treats the transport and chemistry of three tracers: nitrogen oxides (NO + NO<sub>2</sub> + NO<sub>3</sub> + N<sub>2</sub>O<sub>5</sub>), nitric acid (HNO<sub>3</sub>), and peroxyacetylnitrate (PAN). Chemical interconversion rates among the three tracers, as well as intra-conversions among the nitrogen oxides, are calculated off-line and are carried in the GCTM as temporally varying, two- and three-dimensional fields (see section 2 of *Kasibhatla et al.* [1993] and section 2 of *Moxim et al.* [1996] for details). The one exception is the thermal decomposition rate of PAN, which is calculated on-line in the model as a function of the local temperature. Dry deposition fluxes of NO<sub>x</sub>, HNO<sub>3</sub>, and PAN over land and of HNO<sub>3</sub> over oceans, ice, and snow assume a balance between surface deposition and the turbulent flux in the bottom half of the lowest model level [see *Kasibhatla et al.*, 1993, equation 2.2] and use measured depo-

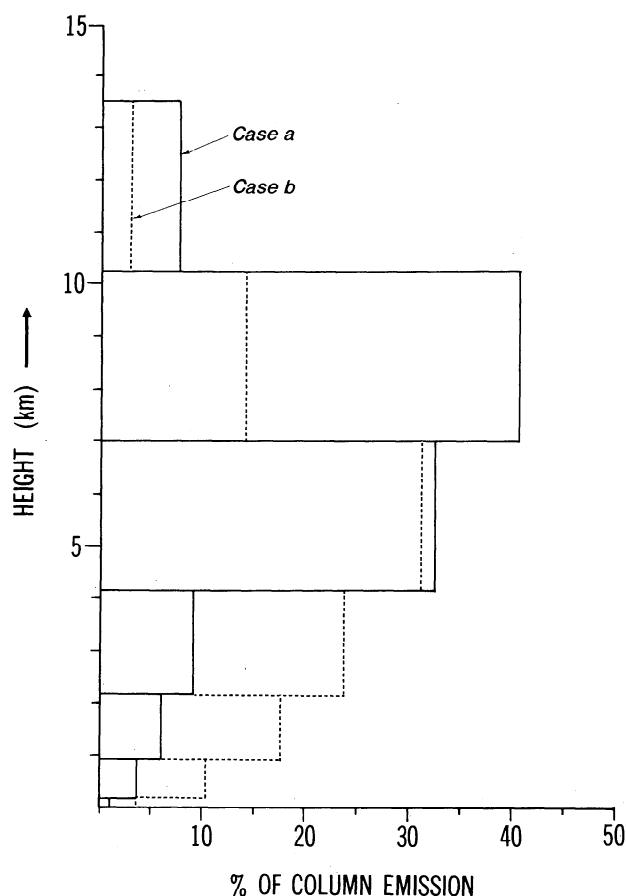


Figure 3. Vertical distribution of the lightning production of NO<sub>x</sub> during deep convection. The dashed line represents case b with CG NO<sub>x</sub> production = 10xIC NO<sub>x</sub> production. The solid line is for case a with CG = IC.

sition velocities of individual reactive nitrogen species (see section 3 of *Kasibhatla et al.* [1993] for details). The removal of HNO<sub>3</sub> by precipitation is calculated using the local precipitation rate, and the wet removal tendency is proportional to the local tracer mixing ratio (see section 2 of *Kasibhatla et al.* [1991] for details).

Along with the natural lightning source of NO<sub>x</sub> being developed in this paper, the model incorporates five other sources: (1) emissions of 21.4 Tg N/yr from surface fossil fuel combustion [*Levy and Moxim* [1989] updated with the GEIA Project [*Benkovitz et al.*, 1996]; (2) aircraft traffic emissions of 0.45 Tg N/yr [*Kasibhatla*, 1993; *Wuebbles et al.*, 1993]; (3) biomass-burning emissions of 8.5 Tg N/yr [*Levy et al.*, 1991], updated by a reduction factor of 0.7 for emissions from the savannas of northern Africa [*Delmas et al.*, 1995]; (4) primarily natural NO<sub>x</sub> emissions from soil of 5.5 Tg N/yr [*Yienger and Levy*, 1995], updated by a reduction factor of 0.1 for emissions from the savannas of northern Africa [*Le Roux et al.*, 1995]; and (5) the injection of 0.65 Tg N/yr of primarily natural stratospheric NO<sub>y</sub> from the stratosphere [*Kasibhatla et al.*, 1991].

#### 3.2. Empirical Global Scaling Factor

In order to determine the global empirical scaling factor, we need global simulations of reactive nitrogen species for two source conditions: (1) a simulation employing all five non-

lightning sources of tropospheric NO<sub>x</sub>; and (2) a second simulation that produces NO<sub>x</sub> and NO<sub>y</sub> levels from the lightning source, scaled to an arbitrary global amount, in our case 1 Tg N/yr.

The determination of the global scaling factor is summarized in Table 2. From left to right are the observed values for NO<sub>x</sub> or NO<sub>y</sub> from regions where lightning plays an important role, the simulated values for the same locations using the five nonlightning sources of NO<sub>x</sub>, the residual (observed minus simulated five source) values that must be explained by lightning, the simulated contribution from a 1 Tg N/yr global lightning source, and the actual global lightning source required to bring a complete six-source simulation into agreement with the observations. We generate median values for the detailed observations in Table 2, while for the sparser data we simply give the range of the data (depicted by brackets). The binning of observed data by altitude was dictated by the model's vertical standard pressure layers as follows: 190 mbar implies a range of 150 to 241 mbar, 315 implies 241-412 mbar, and 500 implies 412-607 mbar. The simulated me-

dian values were generated by sampling all the grid boxes that a flight path passed through over the given time period of the expedition.

The first three missions, STEP, STRATTOZ III and CITE 2 (acronyms are identified in the footnote to Table 2), were the only data sets available when *Levy et al.* [1992] used the case a vertical distribution to arrive at a preliminary estimate of 1-4 Tg N/yr for the global lightning source. With the case b vertical distribution, which is a lower limit on the emission of NO<sub>x</sub> in the upper troposphere, the preliminary estimated range would have risen to 2-6 Tg N/yr. Recently, extensive aircraft measurements of NO<sub>x</sub> from the TRACE-A, PEMwest-A and New Mexico missions have become available, and we find, with the exception of the 315 mbar data over New Mexico, that they all require a global lightning source in the range of 3-6 Tg N/yr. The large majority of the observations require a source in the range of 3-5 Tg N/yr. A more detailed examination of the 315 mbar data over New Mexico shows a bimodal distribution with a small peak at 60-100 pptv and a larger peak at 180-240 pptv. Clearly, the

**Table 2.** Estimated Global Lightning Emissions of NO<sub>x</sub> and NO<sub>y</sub>

Mission <sup>a</sup> and Location	Month	Pressure, mbar	Species	Observed, pptv	Simulated, <sup>b</sup> pptv	Observed Minus Simulated, <sup>a</sup> pptv	Lightning Contribution, pptv/(TgN/yr)	Required Lightning Source, TgN/yr
STEP, <sup>c</sup> Darwin, Australia	Jan.	200	NO <sub>y</sub>	[340 - 420]	119	[221-301]	77	[2.8 - 3.8]
STRATTOZ III <sup>d</sup> Dakar, Senegal	June	190	NO <sub>x</sub>	[100 - 175]	61	[39 - 114]	27	[1.4 - 4.2]
CITE2, <sup>e,f</sup> east N. Pacific (~40°N)	Aug.	500	NO <sub>x</sub>	31	13	18	3	6
			NO <sub>y</sub>	298	219	79	36	2.2
TRACE-A, <sup>g</sup> S. Atlantic (0°-30°S)	Oct.	190	NO <sub>x</sub>	200	69	131	25	5.3
		315	NO <sub>x</sub>	134	56	78	18	4.3
		500	NO <sub>x</sub>	66	38	28	7	4
PEMwest-A <sup>h</sup> west N. Pacific (0°25°N)	Oct.	190	NO <sub>x</sub>	62	20	42	12	3.5
		315	NO <sub>x</sub>	51	9	42	8	5.25
		500	NO <sub>x</sub>	26	11	15	4	3.75
New Mexico <sup>i</sup>	July, Aug.	190	NO <sub>x</sub>	293	237	56	15	3.8
		315	NO <sub>x</sub>	215	48	167	8	21
		500	NO <sub>x</sub>	84	26	58	10	5.8

<sup>a</sup> Mission acronyms are STEP, Stratosphere-Troposphere Exchange Project; STRATTOZ, Stratospheric Ozone Experiment; CITE, Chemical Instrumentation Test and Evaluation; TRACE-A, Transport and Atmospheric Chemistry Near the Equator-Atlantic; PEMwest, Pacific Exploratory Mission-west.

<sup>b</sup> Simulated values for the five nonlightning sources of NO<sub>x</sub>.

<sup>c</sup> Murphy et al. [1993].

<sup>d</sup> Drummond et al. [1988].

<sup>e</sup> Carroll et al. [1990].

<sup>f</sup> Hübler et al. [1992].

<sup>g</sup> Smyth et al. [1996].

<sup>h</sup> Bradshaw (private communication, 1994).

<sup>i</sup> Ridley et al. [1994].

simulation misses the higher peak. This may be due to a model deficiency in lightning in the region, a particular transport situation that is not properly simulated, or aliased data due to limited sampling.

### 3.3. Perspective on Uncertainty

While we have chosen a most probable range of 3-5 Tg N/yr, there are a number of uncertainties in both the analysis and the actual measurements that could both raise and lower the estimated global source strength.

First, there is the suspicion [Crawford *et al.*, 1996; B. Ridley, private communication, 1995; J. Bradshaw, private communication, 1995; D.D. Davis, private communication, 1995] that a number of the NO<sub>x</sub> measurements in the upper

troposphere, because of discrepancies between observed and theoretical NO/NO<sub>2</sub> ratios, may be an overestimate. As a check, we have compared our simulations with calculated NO<sub>x</sub> from the PEMwest-A expedition that are based on measured NO and O<sub>3</sub> [Crawford *et al.*, 1996]. We find that while these NO<sub>x</sub> values give lower estimates of the global source strength (~3 Tg N/yr), they still fall in the same general range.

A potentially significant source of uncertainty is our use of NO<sub>x</sub>, with its implicit reliance on our calculated OH fields, to empirically scale the source. For example, a systematic 50% increase in the upper tropospheric OH mixing ratios would lead to an approximate factor of 2 increase in the required global lightning NO<sub>x</sub> source (6-10 Tg N/yr). While we have previously compared our OH-based CH<sub>3</sub>CCl<sub>3</sub> atmospheric lifetime to the observed value (see Kasibhatla *et al.* [1993] for

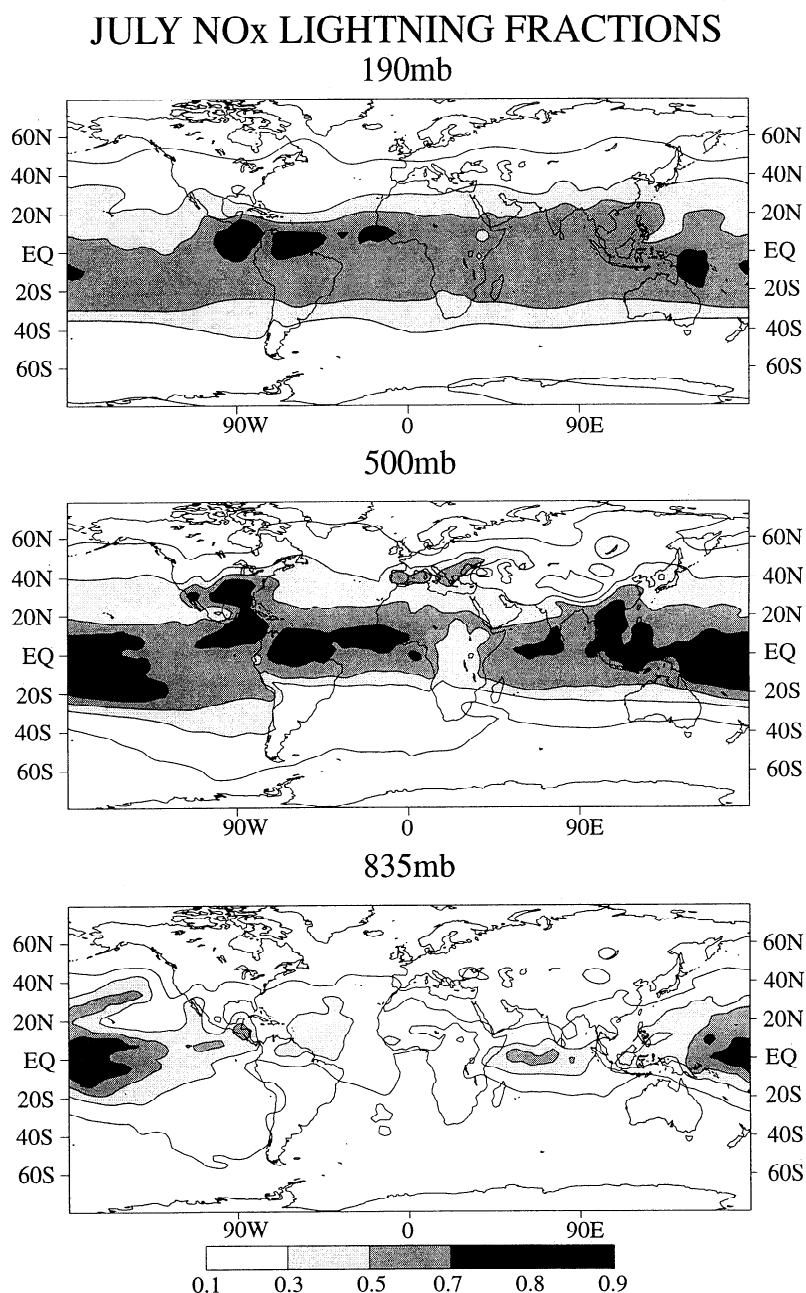


Figure 4. July ratios of simulated monthly mean NO<sub>x</sub> produced by lightning divided by the monthly mean NO<sub>x</sub> levels from all six sources. These ratios or fractions are shown for 190 mbar, 500 mbar and 835 mbar pressure levels.

details), this applies primarily to the lower half of the troposphere because of the large activation energy for CH<sub>3</sub>CCl<sub>3</sub> oxidation. However, our upper tropospheric OH is in reasonable agreement with other calculations [Kasibhatla *et al.*, 1991].

While the use of NO<sub>y</sub> observations, rather than NO<sub>x</sub>, for the empirical scaling would avoid most of the OH uncertainty, there is currently a great deal of uncertainty in the aircraft measurements of NO<sub>y</sub> [Crosley, 1996]. If the sum of the principal measured species (NO<sub>x</sub> + HNO<sub>3</sub> + PAN) is used, the resulting range (1.5-6.5 Tg N/yr) is quite similar to that determined with NO<sub>x</sub>. On the other hand, using directly measured NO<sub>y</sub> leads to a much wider and less certain range of values with a range of 0-18 Tg N/yr and a mean and standard deviation of 10 Tg N/yr and 6 Tg N/yr, respectively.

Another source of uncertainty is the model's simulation of convective transport (for details, see Appendix A of Levy *et*

*al.* [1982], and section 2 of Kasibhatla *et al.* [1993]). If the model underestimates convective transport from the atmospheric boundary layer (ABL), it will also underestimate the contribution of the large surface sources to NO<sub>x</sub> levels in the upper troposphere. The correct convective transport would then require a reduction in the already small (3-5 Tg N/yr) global lightning source. If, on the other hand, convective transport is overestimated, the reverse is true. As an upper limit, we could assume that none of the surface sources contribute to the NO<sub>x</sub> levels in Table 2. This could raise the range of the global source strength as high as 4-9 Tg N/yr.

Although lightning has a strong diurnal dependence in the real world, our simulated source has no diurnal structure. However, by tying our simulated NO<sub>x</sub> emission to the model's vertical instability, which is observed to be highly correlated with lightning in the real world, we do keep the NO<sub>x</sub> emission strongly correlated with the model's upward vertical motion

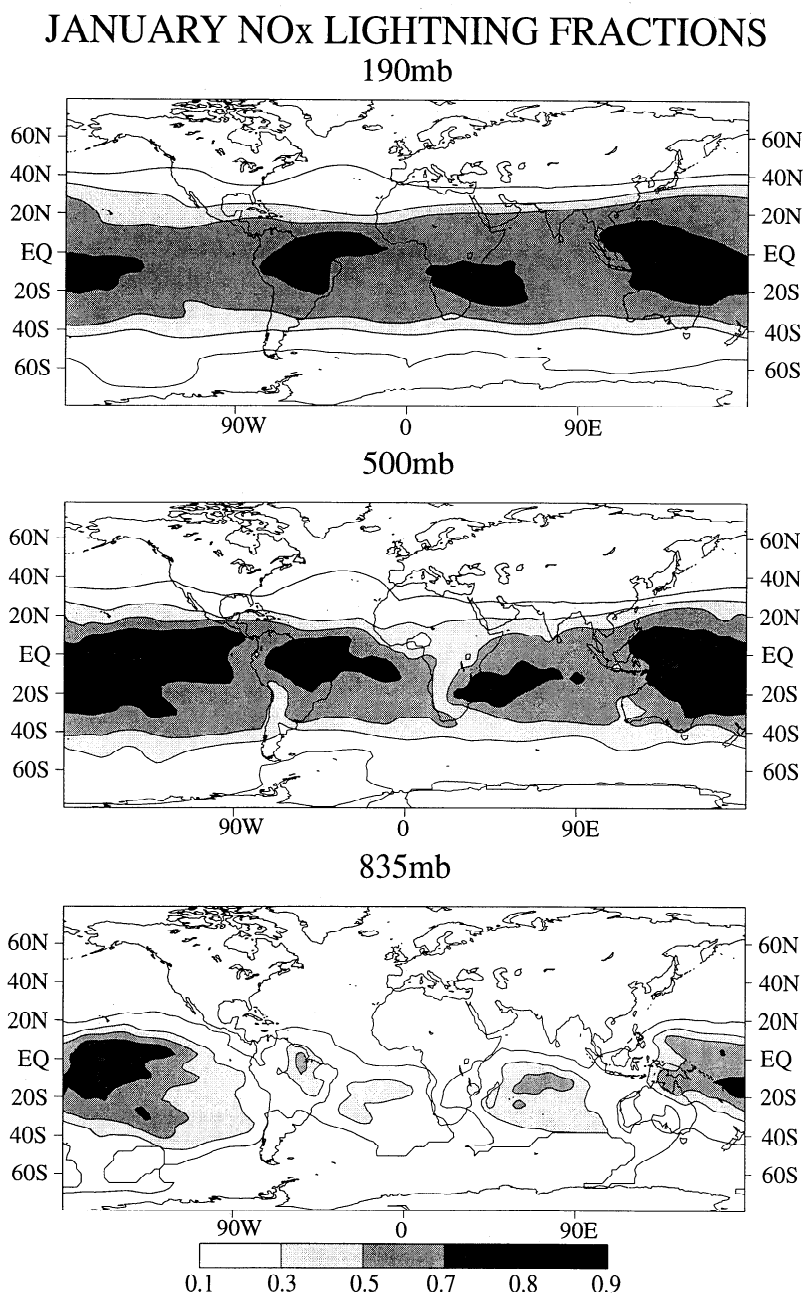


Figure 5. The same ratios as in Figure 4, except for January monthly means.



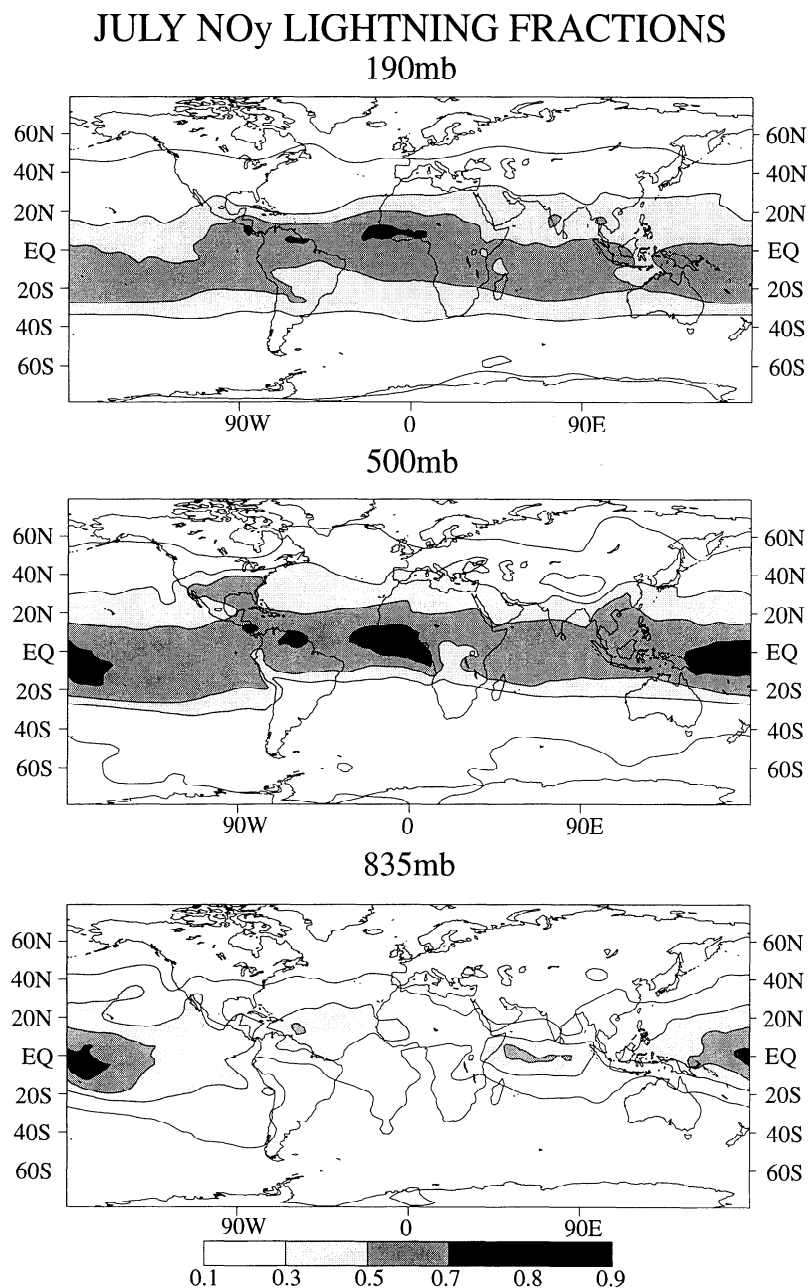


Figure 6. July ratios of simulated monthly mean NO<sub>y</sub> produced by lightning divided by the monthly mean NO<sub>y</sub> levels from all six sources. These ratios or fractions are shown for 190 mbar, 500 mbar and 835 mbar pressure levels.

and mixing. A previous simulation, which ignored this strong correlation between lightning and upward vertical motion, underestimated NO<sub>x</sub> in the upper troposphere by 30% or more. While both the neglected diurnal fluctuations in temperature and systematic errors in the model's temperature field may affect PAN lifetimes in the upper troposphere, PAN chemistry itself has only a small impact on NO<sub>x</sub> levels in that region [Moxim *et al.*, 1996].

Considering all these possible uncertainties, it would appear that our analysis arrives at a clear upper limit of 10 Tg N/yr for the global source strength. Taking a completely different approach, Lawrence *et al.* [1995] have arrived at a range of 1-8 Tg N/yr for the global source of lightning NO<sub>x</sub>. They combine a reanalysis of in situ observations and laboratory studies of NO<sub>x</sub> emissions by lightning flashes with a rela-

tively crude estimate of global flash frequency. In a third approach, C. Price (private communication, 1995) uses International Satellite Cloud Climatology Project (ISCCP) observed clouds and theoretical and empirical relations between cloud properties and flash frequency to derive detailed maps of global flash frequency. These are then combined with a relatively crude estimates of NO<sub>x</sub> production by lightning flashes to arrive at a global budget of 10-15 Tg N/yr. Just recently, Kumar *et al.* [1995] combined satellite observations of global thunderstorm activity and the formula for NO<sub>x</sub> production per flash developed by Borucki and Chameides [1984] to arrive at a global source of 2 Tg N/yr. All the approaches have different weaknesses and different strengths. Nonetheless, all give global budgets in the same general range (1-15 Tg N/yr) with enough uncertainty to explain much of the remaining difference.

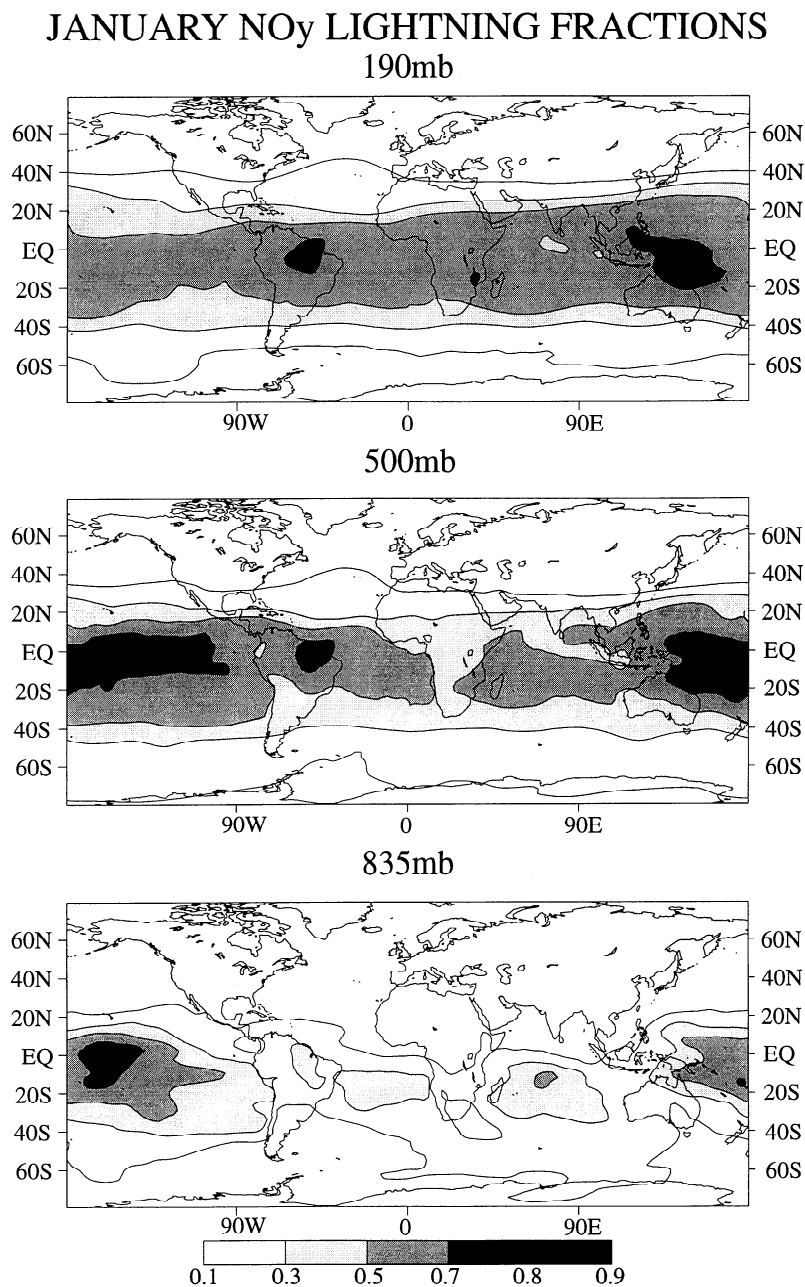


Figure 7. The same ratios as in Figure 6, except for January monthly means.

#### 4. Impact of Lightning on Tropospheric $\text{NO}_x$ and $\text{NO}_y$ [ $\text{NO}_x + \text{HNO}_3 + \text{PAN}$ ]

While lightning flashes may only provide  $\sim 10\%$  of the  $\sim 40 \text{ Tg N/yr}$  of  $\text{NO}_x$  currently emitted into the troposphere, they release  $\text{NO}_x$  into the free troposphere, where it has a relatively long chemical lifetime and can be rapidly transported. This magnifies its impact relative to the competing surface emissions. In Figures 4 and 5 we show global 190 mbar, 500 mbar and 835 mbar maps of the fraction of simulated  $\text{NO}_x$  produced by lightning for July and January, respectively. We chose a conservative lower limit of  $3 \text{ Tg N/yr}$  for the global lightning source strength in these calculations.

Throughout the tropics and subtropics, lightning is the major source of  $\text{NO}_x$  in the upper half of the troposphere, while still making a significant contribution to  $\text{NO}_x$  levels in the

lower troposphere over the remote oceans, where  $\text{NO}_x$  levels are already very low ( $< 10 \text{ pptv}$ ). It is the most dominant in the middle troposphere, particularly during July. In the upper half of the troposphere, lightning makes significant contributions up to  $40^\circ\text{N}$  and  $40^\circ\text{S}$  in their respective summers, is a particularly important source over the continents during summertime convection, and contributes a major fraction over the remote oceans throughout the year. While signs of the convectively active regions appear in the upper troposphere, the impact of lightning is relatively zonal as a result of both the relatively long chemical lifetime of  $\text{NO}_x$  in that region and the rapid transport by the stronger middle and upper tropospheric horizontal winds.

Fractions of simulated  $\text{NO}_y$  resulting from the lightning emissions are shown in Figures 6 and 7. They are qualitatively similar to the  $\text{NO}_x$  fractions shown in Figures 4 and 5 with

lightning being the dominant source of NO<sub>y</sub> in the tropical mid and upper troposphere and in the tropical lower troposphere over the oceans. However, the percentage of NO<sub>y</sub> resulting from the lightning source is generally 10-20% smaller than the NO<sub>x</sub> percentage in the tropical troposphere, particularly over the ocean, where lightning is the only in situ source. It appears that NO<sub>y</sub>, primarily as PAN and HNO<sub>3</sub>, is more readily transported from the surface sources to the free troposphere than is NO<sub>x</sub>, while there is already a direct local source of NO<sub>x</sub> in that region. Therefore we believe that any analysis of NO<sub>x</sub> source contributions that focuses solely on NO<sub>y</sub> will underestimate lightning's contribution to NO<sub>x</sub> and therefore indirectly underestimate its impact on tropospheric ozone chemistry. It should be further noted that our simulations find lightning generally supplying less than 10% of the NO<sub>x</sub> and NO<sub>y</sub> in the troposphere poleward of 50°N and 50°S during both summer and winter.

## 5. Summary and Conclusions

By combining a GCM's convection statistics, empirical relationships and observations of lightning origination and CG : IC flash ratios, and some simplifying assumptions about NO<sub>x</sub> formation by lightning, we are able to generate a "best-estimate" three-dimensional, time-dependent source function for lightning NO<sub>x</sub>. Further, we find that a global source strength ranging from 2 to 6 Tg N/yr with a most probable range of 3-5 Tg N/yr is sufficient to explain most levels of NO<sub>x</sub> measured in the middle and upper troposphere of the tropics and subtropics. With this approach, the global magnitude of the lightning source is constrained by observed levels of NO<sub>x</sub>, while the temporal and spatial distributions of the source are under the control of the parent GCM. Some uncertainties in measured NO<sub>2</sub> in the upper troposphere would support the lower end of the range, while other uncertainties in simulated OH and convective transport could support an upper limit of 10 Tg N/yr. However, even for a global source of 3 Tg N/yr, we find that NO<sub>x</sub> emissions from lightning are the dominant source of tropospheric NO<sub>x</sub> and NO<sub>y</sub> in the upper half of the tropical and subtropical troposphere.

**Acknowledgments.** We wish to acknowledge a number of helpful discussions with C. Price; to thank A. Broccoli, L. Donner, J.D. Mahlman, and two anonymous reviewers for their insightful comments; to gratefully acknowledge the merged data sets provided by Georgia Institute of Technology with the financial aid of NASA's SASS and GTE research programs; to individually thank D. Murphy, D.D. Davis, B. Ridley, J. Walega, S. Sandholm, and J. Bradshaw for providing most of the processed measurement data used in Table 2; and to thank A.I. Hirsch for both gathering the simulated and observed data and performing the statistical analysis on them. P.S. Kasibhatla was funded by the Atmospheric Chemistry Project of the NOAA Climate and Global Change Program under grant NA36GP0250 and by the National Science Foundation under grant ATM-9213643.

## References

- Beck, J. P., C.E. Reeves, F.A.A.M. de Leeuw, and S.A. Penkett, The effect of aircraft emissions on tropospheric ozone in the northern hemisphere, *Atmos. Environ., Part A26*, 17-29, 1992.
- Benkovitz, C.M., J. Pacyna, M.T. Scholtz, L. Tarrason, J. Dignon, E.C. Voldner, P.A. Spiro, J.A. Logan, and T.E. Graedel, Global gridded inventories of anthropogenic emissions of sulfur and nitrogen, *J. Geophys. Res.*, in press, 1996.
- Borucki, W.J., and W.L. Chameides, Lightning: Estimates of the rates of energy dissipation and nitrogen fixation, *Rev. Geophys.*, 22, 363-372, 1984.
- Brooks, C.E.P., The distribution of thunderstorms over the globe, *Geophys. Mem. London*, 24, 147-164, 1925.
- Carroll, M.A., et al., Aircraft measurements of NO<sub>x</sub> over the eastern Pacific and continental United States and implications for ozone production, *J. Geophys. Res.*, 95, 10,205-10,233, 1990.
- Chameides, W.L., and J.C.G. Walker, A photochemical theory of tropospheric ozone, *J. Geophys. Res.*, 78, 8751-8760, 1973.
- Cooray, V., Energy dissipation in lightning flashes, *J. Geophys. Res.*, in press, 1996.
- Crawford, J., et al., Photostationary state analysis of the NO<sub>2</sub>-NO system based on airborne observations from the western and central North Pacific, *J. Geophys. Res.*, 101, 2053-2072, 1996.
- Crosley, D.R., NO<sub>y</sub> Blue Ribbon panel, *J. Geophys. Res.*, 101, 2049-2052, 1996.
- Crutzen, P. J., Photochemical reaction initiated by and influencing ozone in unpolluted tropospheric air, *Tellus*, 26, 45-55, 1974.
- Davis, D.D., J.D. Bradshaw, M.O. Rodgers, S.T. Sandholm, and S. KeSheng, Free tropospheric and boundary layer measurements of NO over the central and eastern North Pacific Ocean, *J. Geophys. Res.*, 92, 2049-2070, 1987.
- Delmas, R., J.P. Lacaux, J.C. Menaut, L. Abbadie, X. Le Roux, G. Helas, and J. Lobert, Nitrogen compound emission from biomass burning in tropical African savanna FOS/DECAFE 1991 Experiment (Lamto, Ivory Coast), *J. Atmos. Chem.*, 22, 175-193, 1995.
- Dignon, J., J.E. Penner, C.S. Atherton, and J.J. Walton, Atmospheric reactive nitrogen: A model study of natural and anthropogenic sources and the role of microbial soil emissions, paper presented at CHEMRAWN VII World Conference on Atmospheric Chemistry, American Chemical Society, Baltimore, Md., 1992.
- Drummond, J.W., D.H. Ehhalt, and A. Volz, Measurements of nitric oxide between 0-12 km altitude and 67°N to 60°S latitude obtained during STRATOZ III, *J. Geophys. Res.*, 93, 15,831-15,849, 1988.
- Fehsenfeld, F.C., D.D. Parrish, and D.W. Fahey, The measurement of NO<sub>x</sub> in the non-urban troposphere, in *Tropospheric Ozone*, edited by I.S.A. Isaksen, pp. 185-216, D. Reidel, Norwell, Mass., 1988.
- Franzblau, E., and C.J. Popp, Nitrogen oxides produced from lightning, *J. Geophys. Res.*, 94, 11,089 - 11,104, 1989.
- Galloway, J.N., H. Levy II, and P.S. Kasibhatla, Year 2020: Consequences of population growth and development on deposition of oxidized nitrogen, *Ambio*, 23, 120-123, 1994.
- Galloway, J.N., D.L. Savoie, W.C. Keene, and J.M. Prospero, The temporal and spatial variability of scavenging ratios for nss sulfate, nitrate, methanesulfonate and sodium in the atmosphere over the North Atlantic Ocean, *Atmos. Environ., Part A27*(2), 235-250, 1993.
- Goodman, S.J., and H.J. Christian, Global observations of lightning, in *Atlas of Satellite Observations Related to Global Change*, edited by R.J. Gurney, J.L. Foster, and C.L. Parkinson, pp. 191-219, Cambridge Univ. Press, New York, 1993.
- Goodman, S.J., and D.R. MacGorman, Cloud-to-cloud lightning activity in mesoscale convective complexes, *Mon. Weather Rev.*, 114, 2320-2328, 1986.
- Hameed, S., and J. Dignon, Changes in the geographical distributions of global emissions of NO<sub>x</sub> and SO<sub>x</sub> from fossil fuel combustion between 1966 and 1980, *Atmos. Environ.*, 22, 441-449, 1988.
- Hameed, S., O.G. Paidoussis, and R.W. Stewart, Implications of natural sources for the latitude gradient of NO<sub>y</sub> in the unpolluted troposphere, *Geophys. Res. Lett.*, 8, 591-594, 1981.
- Hao, W.M., M.H. Liu, and P.J. Crutzen, Estimates of annual and regional releases of CO<sub>2</sub> and other trace gases to the atmosphere from fires in the tropics, based on FAO statistics from the period 1975-1980, paper presented at Third International Symposium on Fire Ecology, Freiburg Univ., Freiburg, Germany, 1989.
- Holmes, C.R., M. Brook, P. Krehbiel, and R.A. McCarty, On the power spectrum and mechanism of thunder, *J. Geophys. Res.*, 76, 2106-2115, 1971.
- Hübner, G., D.W. Fahey, B.A. Ridley, G.L. Gregory, and F.C. Fehsenfeld, Airborne measurements of total reactive odd nitrogen (NO<sub>y</sub>), *J. Geophys. Res.*, 97, 9833-9850, 1992.
- Kasibhatla, P.S., NO<sub>y</sub> from sub-sonic aircraft emissions: A global

- three-dimensional model study, *Geophys. Res. Lett.*, *20*, 1707-1710, 1993.
- Kasibhatla, P.S., H. Levy II, W.J. Moxim, and W.L. Chameides, The relative impact of stratospheric photochemical production on tropospheric NO<sub>y</sub> levels: A model study, *J. Geophys. Res.*, *96*, 18,631-18,646, 1991.
- Kasibhatla, P.S., H. Levy II, and W.J. Moxim, Global NO<sub>x</sub>, HNO<sub>3</sub>, PAN, and NO distributions from fossil-fuel combustion emissions: A model study, *J. Geophys. Res.*, *98*, 7165-7180, 1993.
- Kowalczyk, M., and E. Bauer, Lightning as a source of NO<sub>x</sub> in the troposphere, *Tech. Rep. FAA-EE-82-4*, 76 pp., Inst. for Defense Anal., Alexandria, Va., 1982.
- Kumar, P.P., G.K. Manohar, and S.S. Kandalgaonkar, Global distribution of nitric oxide produced by lightning and its seasonal variation, *J. Geophys. Res.*, *100*, 11,203-11,208, 1995.
- Lawrence, M.G., W.L. Chameides, P.S. Kasibhatla, H. Levy II, and W. Moxim, Lightning and atmospheric chemistry: The rate of atmospheric NO production, in *Handbook of Atmospheric Electrodynamics*, vol. 1, edited by H. Volland, pp. 189-202, CRC Press, Boca Raton, Fl., 1995.
- Le Roux, X., L. Abbadie, R. Lensi, and D. Serca, Emission of nitrogen monoxide from African tropical ecosystems: Control of emission by soil characteristics in humid and dry savannas of West Africa, *J. Geophys. Res.*, *100*, 23,133-23,142, 1995.
- Levy, H. II, Normal atmosphere: Large radical and formaldehyde concentrations predicted, *Science*, *173*, 141-143, 1971.
- Levy, H. II, and W.J. Moxim, Simulated global distribution and deposition of reactive nitrogen emitted by fossil fuel combustion, *Tellus*, *41*, 256-271, 1989.
- Levy, H. II, J.D. Mahlman, and W.J. Moxim, Tropospheric N<sub>2</sub>O variability, *J. Geophys. Res.*, *87*, 3061-3080, 1982.
- Levy, H. II, J.D. Mahlman, W.J. Moxim, and S.C. Liu, Tropospheric ozone: The role of transport, *J. Geophys. Res.*, *90*, 3753-3772, 1985.
- Levy, H. II, W.J. Moxim, P.S. Kasibhatla, and J.A. Logan, The global impact of biomass burning on tropospheric reactive nitrogen, in *Global Biomass Burning: Atmospheric, Climatic, and Biospheric Implications*, edited by J.S. Levine, pp. 363-369, MIT Press, Cambridge, Mass., 1991.
- Levy, H. II, P.S. Kasibhatla, and W.J. Moxim, Global tropospheric NO<sub>x</sub> (The role of lightning), paper presented at CHEMRAWN VII World Conference on Atmospheric Chemistry, American Chemical Society, Baltimore, Md., 1992.
- Liaw, Y., D.L. Sisterson, and N.L. Miller, Comparison of field, laboratory, and theoretical estimates of global nitrogen fixation by lightning, *J. Geophys. Res.*, *95*, 22,489-22,494, 1990.
- Lin, X., M. Trainer, and S.C. Liu, On the nonlinearity of the tropospheric ozone production, *J. Geophys. Res.*, *93*, 15,879-15,888, 1988.
- Liu, S.C., M. McFarland, D. Kley, O. Zafiriou, and B. Huebert, Tropospheric NO<sub>x</sub> and O<sub>3</sub> budgets in the equatorial Pacific, *J. Geophys. Res.*, *88*, 1360-1368, 1983.
- Logan, J.A., Nitrogen oxides in the troposphere: Global and regional budgets, *J. Geophys. Res.*, *88*, 10,785-10,807, 1983.
- Mahlman, J.D., and W.J. Moxim, Tracer simulation using a global general circulation model: Results from a midlatitude instantaneous source experiment, *J. Atmos. Sci.*, *35*, 1340-1374, 1978.
- Manabe, S., and J.L. Holloway Jr., The seasonal variation of the hydrologic cycle as simulated by a global model of the atmosphere, *J. Geophys. Res.*, *80*, 1617-1649, 1975.
- Manabe, S., D.G. Hahn, and J.L. Holloway Jr., The seasonal variation of the tropical circulation as simulated by a global model of the atmosphere, *J. Atmos. Sci.*, *31*, 43-83, 1974.
- Moxim, W.J., H. Levy II, and P.S. Kasibhatla, Simulated global tropospheric PAN: Its transport and impact on NO<sub>x</sub>, *J. Geophys. Res.*, *101*, 12,621-12,638, 1996.
- Moxim, W.J., H. Levy II, P.S. Kasibhatla, and W.L. Chameides, The impact of anthropogenic and natural NO<sub>x</sub> sources on the global distribution of tropospheric reactive nitrogen and the net chemical production of ozone (abstract), *Eos Trans. AGU*, *75*(44), Fall Meet. Suppl., 135, 1994.
- Müller, J.-F., Geographical distribution and seasonal variation of surface emissions and deposition velocities of atmospheric trace gases, *J. Geophys. Res.*, *97*, 3787-3804, 1992.
- Murphy, D.M., D.W. Fahey, M.H. Proffitt, S.C. Liu, K.R. Chan, C.S. Eubank, S.R. Kawa, and K.K. Kelly, Reactive nitrogen and its correlation with ozone in the lower stratosphere and upper troposphere, *J. Geophys. Res.*, *98*, 8751-8773, 1993.
- Orville, R.E., and R.W. Henderson, Global distribution of midnight lightning: September 1977 to August 1978, *Mon. Weather Rev.*, *114*, 2640-2653, 1986.
- Orville, R.E., and D.W. Spencer, Global lightning flash frequency, *Mon. Weather Rev.*, *107*, 934-943, 1979.
- Penner, J.E., C.S. Atherton, J. Dignon, S.J. Ghan, J.J. Walton, and S. Hameed, Tropospheric nitrogen: A three-dimensional study of sources, distributions, and deposition, *J. Geophys. Res.*, *96*, 959-990, 1991.
- Price, C., and D. Rind, A simple parameterization for calculating global lightning distributions, *J. Geophys. Res.*, *97*, 9919-9933, 1992.
- Price, C., and D. Rind, What determines the cloud-to-ground lightning fraction in thunderstorms?, *Geophys. Res. Lett.*, *20*, 463-466, 1993.
- Proctor, D.E., Regions where lightning flashes began, *J. Geophys. Res.*, *96*, 5099 - 5112, 1991.
- Ridley, B.A., J.G. Walega, J.E. Dye, and F.E. Grahek, Distribution of NO, NO<sub>x</sub>, NO<sub>y</sub>, and O<sub>3</sub> to 12 km altitude during the summer monsoon season over New Mexico, *J. Geophys. Res.*, *99*, 25,519-25,534, 1994.
- Smyth, S.B., et al., Factors influencing the upper free tropospheric distribution of reactive nitrogen over the South Atlantic during the TRACE-A experiment, *J. Geophys. Res.*, in press, 1996.
- Trainer, M., et al., Observations and modeling of the reactive nitrogen photochemistry at a rural site, *J. Geophys. Res.*, *96*, 3045-3063, 1991.
- Turman, B.N., and B.C. Edgar, Global lightning distribution at dawn and dusk, *J. Geophys. Res.*, *87*, 1191-1206, 1982.
- Wuebbles, D.J., D. Maiden, R.K. Seals Jr., S.L. Baughcum, M. Metwally, and A. Mortlock, Emissions scenarios development: Report of the Emissions Scenarios Committee, in *The Atmospheric Effects of Stratospheric Aircraft: A Third Program Report*, edited by R. S. Stolarski and H. L. Wesoky, *NASA Ref. Publ.*, *1313*, 1993.
- Yienger, J., and H. Levy II, Empirical model of global soil-biogenic NO<sub>x</sub> emissions, *J. Geophys. Res.*, *100*, 11,447-11,464, 1995.

P.S. Kasibhatla, MCNC, Environmental Programs, Research Triangle Park, NC 27709.

H. Levy II and W.J. Moxim, NOAA Geophysical Fluid Dynamics Laboratory, P.O. Box 308, Princeton University, Princeton, NJ 08542. (e-mail: hl@gfdl.gov)

(Received July 16, 1995; revised June 28, 1996; accepted June 28, 1996.)